



Biogenic isoprenoid emissions under drought stress: Different responses for isoprene and terpenes

Boris Bonn¹, Ruth-Kristina Magh¹, Joseph Rombach¹, Jürgen Kreuzwieser¹

¹Chair of Ecosystem Physiology/Chair of Tree Physiology, Faculty of Environment and Natural Resources, Albert-Ludwigs-Universität, Georges-Köhler-Allee 053, D-79110 Freiburg i.Br., Germany

Correspondence to: Boris Bonn (boris.bonn@ctp.uni-freiburg.de)

Abstract. Emissions of volatile organic compounds (VOCs) by biogenic sources depend on different environmental conditions. Besides temperature and photosynthetic active radiation (PAR), the available soil water can be a major factor, controlling the emission flux. This factor is expected to become more important under future climate conditions including prolonged drying-wetting cycles. In this paper we use results of available studies on different tree types to set up a parameterization describing the influence of soil water availability (SWA) on different isoprenoid emission rates. Investigating SWA effects on isoprene (C_5H_8), mono- ($C_{10}H_{16}$) and sesquiterpene ($C_{15}H_{24}$) emissions separately, it is obvious that different plant processes seem to control the individual emission fluxes providing a measure of plants to react on stresses and to interact. The SWA impact on isoprene emissions is well described by a biological growth type curve, while the sum of monoterpenes displays a hydraulic conductivity pattern reflecting the plants stomata opening. However, emissions of individual monoterpene structures behave differently to the total sum, i.e. the emissions of some increase whereas of others decline at decreasing SWA. In addition to a rather similar behaviour as of monoterpene emissions, total sesquiterpene fluxes of species adapted to drought stress tend to reveal a rise close to the wilting point protecting against oxidative damages. Considering further VOCs too, the total sum of VOCs tends to increase at the start of severe drought conditions until resources decline. On the contrary, OH and ozone reactivity enhance. Based on these observations a set of plant protection mechanism displays for drought stress and implies notable feedbacks on atmospheric processes such as ozone, aerosol particles and cloud properties. With progressing length of drought periods declining storage pools and plant structure effects yield different emission mixtures and strengths. This drought feedback effect is definitely worth consideration in climate feedback descriptions and for accurate climate predictions.

25 1 Introduction

The exchange of biogenic VOCs (E) is known to represent the largest contribution to global carbon flux besides carbon dioxide (CO_2) and methane (CH_4) (IPCC, 2014; Niinemets et al., 2014; Holopainen et al., 2017). The total amount of individual BVOC fluxes, i.e. emission and corresponding deposition rates (exchange = emission+deposition), is linked to their production (*de novo* synthesis or online) and storage (offline) capacities of individual plant types and species (Ghirardo et al., 2010) and is



30 additionally affected by abiotic and biotic conditions. These include the temperatures of vegetation (T_{veg}) and soil (T_{soil}),
photosynthetic active radiation (PAR), ambient CO₂ mixing ratio, defense against herbivores (Manninen et al., 1998) and
reactive air pollutants (Bourtsoukidis et al., 2012, plant-plant communication and competition, fire and drought (Lappalainen
et al., 2009; Penuelas et al., 2010; Guenther et al., 2012). While BVOCs represent a large variability of different structures and
35 species (Goldstein and Galbally, 2007; Laothawornkitkul et al., 2009), it is commonly accepted that isoprene (C₅H₈) and
monoterpenes (C₁₀H₁₆) display the majority (38–50% and 30%, respectively) of total BVOC exchange (1–1.3 Pg yr^{−1})
(Goldstein and Galbally, 2007; Guenther et al., 1995; Guenther et al., 2012), if methane is excluded. The exchange E is
commonly described by the exchange at standard conditions E_0 ($T = 30$ °C) and scaled by factors for individual driving forces
such as temperature (T), light (L) (Guenther et al., 1995; 2006; 2012) or soil water content (SWC), here denoted as SM in the
index in accordance with the formulation of Guenther et al. (2006; 2012):

40

$$E = E_0 \cdot \gamma_T \cdot \gamma_L \cdot \gamma_{CO_2} \cdot \gamma_{SM} \quad (1)$$

Please find an overview of all the abbreviated terms and parameters in Table 1. Some of the scaling factors of driving forces
(γ) for exchange are reasonably well-described regarding temperature and PAR, while other parameters like soil water
45 availability (SWA) are mostly ignored due to a lack of understanding of influencing plant processes, although a simplified
parameterisation exists (Guenther et al., 2012). This neglect is confronted with changing climate conditions such as warming
of 0.15 K/20 years (Schoelzel et al., 2011) with predicted extending drought periods in Central European forest ecosystems
such as the Black Forest in Southern Germany (Keuler et al., 2016; Kreienkamp et al., 2018). So far a single simplified
50 formulation using a linear increase from no emission at the permanent wilting point (PWP) to maximum emission shortly
above this point is commonly applied for different conditions. This is based on an experiment of poplar (Pegoraro et al., 2004a),
analyzing isoprene only. The changing soil water conditions and the resulting change in BVOC exchange fluxes are expected
to influence plant responses and protection capacities (Penuelas et al., 2010; Rennenberg et al., 2006), the exchange following
up ozone formation strength and further climate feedback processes (Bonn et al., 2014). In this study we aim at investigating
55 the individual behaviour of isoprene, mono- (MT) and sesquiterpene (SQT) exchange fluxes and their correlation with SWA
for available tree species to allow identification of processes controlling the emission. As European beech (*Fagus sylvatica*),
which is SWA sensitive (Gessler et al., 2007; Dalsgaard et al., 2011), is one of the most common tree species in Central Europe
and of economic importance (Kändler et al., 2016), we will focus on the impact of the SWA effect on emissions.



2 Materials and methods

2.1 Review of available studies and transfer between different water content parameters used

60 In order to develop an advanced description of limited soil water on BVOC exchange, available studies were collected, focussing on isoprenoid emissions in the context of different drought conditions. These studies include different tree types and several herbs predominantly under controlled conditions and for selected compounds or compound groups (Table 2).

2.2 Adapting available studies to a comparative scheme

65 2.2.1 Different conditions of individual studies

First, available studies on BVOC exchange for different tree species at different soil water conditions have been collected. It is important to note that these studies have been described in various ways using

70 (a) different soil water parameters (SWA, soil water content (SWC) and water matrix potential (ψ_m)),
(b) different plant ages,
(c) different soil types,
(d) different lengths of investigation and time resolutions,
(e) with and without re-watering and
(f) different environments (laboratory, greenhouse and ambient).

The named different parameters complicate a direct comparison and include the assumption of an applicable transfer of
75 laboratory or greenhouse experimental results with predominantly seedlings to ambient conditions, a transfer including notable challenges and questions as discussed e.g. by Niinemets (2010).

2.2.2 Different parameters used for describing the effect of soil water

The plants access to soil water is best described by the accessible water SWA (index '%': fraction of accessible water, index
80 'v': volumetric amount) or by the suction pressure ψ_m . Both parameters denote the soil water status and the ability of a plant to extract water from it (Blume et al., 2010). However, the easiest parameter to quantify soil water conditions by measurement continuously is volumetric SWC (SWC_v). Therefore, SWC_v has so far been used to estimate soil water effects on plants processes e.g. by Guenther et al. (2006, 2012). However, different soil types possess different PWP preventing water to be extracted by the plant below. Without the knowledge of the PWP of the soil investigated the information of SWC_v to describe the plant
85 water access remains incomplete and makes different studies difficult to compare. Therefore, we focus on SWA% as primary parameter for describing the soil water effect and provide a set of equations to transfer between the different quantities. This makes different amounts of soil water comparable for different soil conditions and furthermore allows an easy usage in model studies that formerly used SWC_v (Guenther et al., 2006; 2012). To support this all parameterizations are stated by both, i.e. (a) by SWA% and (b) by SWC_v . The SWA describes the amount of soil water above PWP ($\psi = -4.2$ MPa) up to field capacity



90 (amount of water held by the soil against gravity, FK , $\psi = -0.0063$ MPa), and is called available or net field capacity (nFK) for the corresponding soil type, and which depends on the soil capacity to fix water (van Genuchten, 1980). During short terms SWA can exceed nFK (e.g. after an intense rain fall), but this excess water infiltrates the soil and is not available to the plant thereafter. A list of the different parameters used in the available literature is given and the transfer in between is assumed as (Blume et al., 2010):

95 $SWA\% = SWA_v/nFK = (SWC_v - PWP)/nFK$ (2a)

$SWA_v = SWC_v - PWP$ (2b)

$SWC_v = SWA_v + PWP = SWA\% \cdot nFK + PWP$ (2c)

$nFK = \max(SWA_v) = FK - PWP$ (2d)

$FASW\% = SWC\% = SWC_v/(nFK + PWP)$ (2e)

100 $FASW\%$ and $SWC\%$ abbreviate the volumetric soil water content relative to its maximum value (field capacity FK). Converting water or matrix potential ψ values is a function of the actual soil mixture of clay, sand and silt, i.e. the different corn size distributions/classes and the intercorn spaces available for water storage, which can be described by a water retention curve (van Genuchten diagram (van Genuchten, 1980), see e.g. Blume et al. (2010)):

$SWA\% = ((SWC_{v,r} + (SWC_{v,max} - SWC_{v,r})/(1 + (a \cdot |\psi| \text{ [MPa]} \cdot 10^4)^n)^{1-1/n}) - PWP)/nFK$ (3a)

105 $SWC_v = SWC_{v,r} + (SWC_{v,max} - SWC_{v,r})/(1 + (a \cdot |\psi| \text{ [MPa]} \cdot 10^4)^n)^{1-1/n}$ (3b)

$SWC_{v,r}$ is the residual SWC at completely air dried conditions, $SWC_{v,max}$ is the SWC_v at saturation, a the inverse of the air entry suction and n represents a measure of the pore-size distribution. Representative data for different soil textures can be found e.g. in Leij et al. (1996) and at http://soilphysics.okstate.edu/software/water_conductivity.html (access: 2019-01-17).

2.2.3 Different soil types, corresponding PWP s and FK s

110 PWP and FK values for different soil types were calculated from the articles information based on data summarized by Chen and Dudhia (2001), and their common soil type classification. Different soil types, predominantly expressed by different corn sizes (corn diameter D_p) and pore space volume, available for soil water, can be classified according to the contribution of sand ($0.002 \text{ mm} < D_p < 2 \text{ mm}$), silt ($0.002 \text{ mm} < D_p < 0.050 \text{ mm}$) and clay ($D_p < 0.002 \text{ mm}$). Those mimic the potential of the soil texture to fix water, against which the suction pressure of plants needs to work for extracting soil water. This determines 115 not only the PWP of the corresponding soil, i.e. the point at which a plant is unable to suck out any water of the soil pores, but also the maximum amount of water a soil can hold against gravity (FK or $SWC_{v,max}$). The individual studies published refer to different soil types, PWP s and $SWC_{v,max}$ that need to be considered and included in a more general parameterization. Here, we use the contribution of individual soil types to the mixtures applied in the corresponding studies for calculating the PWP and



the $SWC_{v,max}$. In order to make different soil types and conditions comparable, all soil water describing parameters were
120 converted to $SWA\%$ using PWP and nFK .

As this study is part of a beech – silver fir research project in Southwestern Germany most figures shown are displayed with
two horizontal axes, (i) the reference $SWA\%$ in percentage and (ii) an exemplary SWC_v describing the one at the projects field
site in Freiamt, Black Forest, Southwestern Germany (Magh et al., 2018). This is representative for natural European beech
soil common in Central Europe (Gessler et al., 2007) with a PWP of 4.7% and a nFK of 31.2%. In order to make results
125 applicable to a wider range, any fitted equations take into account the soil properties and are provided for general conditions
as functions of (i) $SWA\%$ (general reference) and of (ii) SWC_v (requires adaptation to local conditions).

2.3 Different fitting approaches and corresponding driving forces

The effect of soil moisture on the emission of BVOCs is described by Guenther et al. (2006; 2012) using three-step pattern:
Assuming (1) no emission below the PWP , (2) a linear increase of emissions between PWP ($\gamma_{SM} = 0$) and $PWP+4$ vol% of
130 SWC_v ($\gamma_{SM} = 1$) and (3) a soil moisture independent emission above. This empirical parameterization was based on isoprene
emission measurements of Canadian black poplar (*Populus deltoides*) at the Biosphere 2 facility (Pegoraro et al., 2004a). A
different suggestion, exponential dependence of emission on SWC_v was published recently by Genard-Zielinski et al. (2018)
for isoprene emissions too but for downy oak (*Quercus pubescens*) instead of black poplar.

For the overall soil moisture dependency of BVOC emissions at standard conditions ($T = 30^\circ\text{C}$) several processes become
135 important depending on the molecular size of the compound, its production and storage behavior as well as its water solubility.

(i) Stomata controlled effect: If the size of the BVOC molecule does not allow penetration of the leaf or needle surface layer
the least barrier between plant and atmosphere are the stomata. Thus, the emission process is controlled by stomatal opening
behaviour of the plant species (Simpson et al., 1985). Low $SWA\%$ and SWC_v causes low ψ - please note the negative scale,
which triggers closure of stomata in order to increase the resistance for water molecules between leaf and atmosphere, helping
140 to avoid loss of water by transpiration. Thus, γ_{SM} alters according to hydraulic conductivity pattern (index 'h') given as

$$\gamma_{SM,h} = a_h + b_h \cdot SWA\% / (c_h + SWA\%) = a_h + b_h \cdot (SWC_v - PWP) / (c_h / nFK + SWC_v - PWP) \quad (4a).$$

The curve starts at a_h , i.e. the residual emitted fraction at PWP and increases to unity as $SWA\%$ reaches 100% at $SWC_{v,max}$ (FK).
Both coefficients b_h and c_h determine the exact shape and slope of increase and are linked via

$$c_h = (b_h + SWC_v(PWP) - 1) \cdot (SWC_{v,max} - PWP) \quad (4b).$$

145 The shape is therefore different to the approach used in the MEGAN formulation (Guenther et al., 2006; 2012) as the effect
sets in already below SWC_{max} .



(ii) Diffusion controlled effect: If the emission may take place at least partially through the *cuticula*, perhaps for smaller chemical species, loss of plant water will cause a bending of the tissue surface. This will increase the cell pressure and influence conditions and forces of contained smaller BVOCs leading to diffusion towards the ambient, i.e. emission. This process acts 150 similar to biological growth processes and can be described by

$$\gamma_{SM,g} = \exp(-\exp(b_g \cdot \exp(1) \cdot (c_g - (SWC_v - PWP)/nFK) + 1)) = \exp(-\exp(b_g \cdot \exp(1) \cdot (c_g - SWA\%) + 1)) \quad (5).$$

Similar as above b_g as well as c_g represent curve shape parameters. The implicit γ_{SM} value at PWP , i.e. a_g , is given by $\exp(-\exp(b_g \cdot \exp(1) \cdot (c_g) + 1))$.

(iii) Water solubility and transport effect: Further important processes as water dependent productivity or transport (e.g. via 155 sap flow) will display either a linear behavior or a mixture of Eqs. 4 and 6. This depends on the limitations in the entire process chain from production, storage, potential transport and emission, which may be controlled by stomata opening or diffusion through the *cuticula*.

(iv) Plant defense or interaction effect: Finally, a rise of BVOC emissions shortly above the PWP is apparent in some MT but mainly SQT related studies. This may be explained by plant defensive strategies such as detoxification and reduction of radical 160 oxidative species (ROS) species, as most of these chemical species possess a high reactivity concerning ozone and radicals. The observations indicate an increase with decreasing $SWA\%$ or SWC_v , until a rapid collapse close to PWP . We consider these observations to appear like a Gamma function type with a maximum near the PWP , i.e. $a \cdot (SWA\% + b)^c \cdot \exp(-d \cdot (SWA\% + b))$ with a set of parameters a , b , c and d characteristic for individual plant species. They may potentially reflect a species ability to respond to oxidative stress.

165 2.4 Exemplary field studies: Application to ambient conditions

2.4.1 Plant nursery, Freiburg

Eleven 8-10 years old *Fagus sylvatica* seedlings were studied in the plant nursery of the Chair of Ecosystem Physiology (48.014695° N, 7.832494° E) of the Albert Ludwigs Universität Freiburg with different soil water potentials, which were determined predawn and during daytime between July 19th and 31st 2018. Six trees served as control plants, which were watered 170 regularly, while rainwater was excluded by self-constructed roofs above the soil for the other five trees. Noteworthy, summer 2018 was extremely dry with less precipitation below 35 mm m⁻² during June and July, which is only one third of the 30 year average (90.5±40.5 mm m⁻², Freiburg airport, distance: ca. 900 m NNW, German Weather Service, ftp://ftp-cdc.dwd.de/pub/CDC/observations_germany/climate/ monthly/kl/) for those two months. Mean SWC_v of control and stressed beeches were approximated by two methods, (i) water potential of the experimental plants was determined with a Scholander 175 pressure chamber (Scholander, 1966) at a cut branch predawn and around noon, and (ii) by SWC_v measurements at a nearby field (ca. 600 m NW) with a similar soil structure (VWC, 10HS, Decagon, Washington, USA). BVOC emission with the



method described by Haberstroh et al. (2018). For this purpose, BVOCs emitted from beech leaves were collected during daytime using air- sampling tubes filled with Tenax (Gerstel). Analysis occurred on GC-MS system (GC model 7890 B, GC System, MS: 5975 C VL MSD with triple-Axis Detector, Agilent Technologies, Waldbronn) equipped with a multipurpose sampler (MPS 2, Gerstel, Mülheim, Germany) (Magh et al., in prep.). More details on the analysis can be found here (Kleiber et al., 2017).

Based on the observed emission rates and corresponding forest air composition, relative changes in OH and ozone reactivity of the emission cocktail observed were derived as follows (Nölscher et al., 2014; Mogensen et al., 2015): The sum of the individual products of emission rates [$\text{molecules m}^{-2} \text{ h}^{-1}$], and their corresponding reaction rate constants [$\text{cm}^3 \text{ molecule s}^{-1}$]
185 was calculated and compared to the related sum of the undisturbed reference trees. This includes the knowledge of a large set of compound reaction rates of which some are not obtainable in the available literature. Those have been approximated using structure activity relationship (SAR) based algorithms developed by Neeb (2000) and McGillen et al., (2011). In order to do so, the molecule of interest was split in its functional groups and the respective coefficients used for the estimate. As this approach is relative (i.e. disturbed to undisturbed trees), emissions of any vertical mixing is unimportant here, but will have to
190 be considered for the detailed atmospheric impact and its range. In this case, it is worth mentioning that forests extend usually to some tenths of kilometers in the Black Forest area and the area of emission can be easily traced back within the next kilometers in distance (unpublished data). This indicates the importance of BVOC emissions on the local atmospheric chemistry.

2.4.2 Black forest conditions at Freiamt

195 SWC_v values were measured at five different depths (5, 10, 25, 50 and 75 cm) with a time resolution of 2h. Sensors were placed at different locations to test the heterogeneity, especially beneath different tree types, i.e. European beech (*Fagus sylvatica*) and Silver fir (*Abies alba*) and in between. For further information on measurements see Magh et al. (in prep.).

In order to approximate ambient SWC_v effects on isoprene and terpene emissions, Eqs. 1, 3, 4 and 6 have been applied to meteorological measurements nearby and SWC_v .

200 **3 Results**

As indicated in section 2.3 we standardized and tested the influence of available soil water on emission rates of isoprene (E_{isop}), MT (E_{MT}) and SQT (E_{SQT}) using different hypotheses, a) a stepwise effect (Guenther et al., 2006), b) a growth rate like behavior (Eq. 5), a) hydraulic conductivity pattern (Eqs. 4a and b) as well as d) a stress defense response of SWA% (lower x-axis) and for comparison the SWC_v for a selected condition (upper horizontal axis).



205 **3.1 Isoprene**

Most studies on plant BVOC emissions affected by limited amounts of soil water investigated isoprene. A summary plot of individual studies rescaled to comparable conditions is provided in Fig. 1. In here the corresponding $SWA\%$ conditions are plotted vs. γ_{SM} . A secondary horizontal axis on the top of Fig. 1 displays typical SWC_v representative for Black Forest conditions at the Freiamt site ($PWP = 4.7$, $nFK = 31.2\%$, soil: loamy sand; Magh et al., 2018). These conditions are similar to 210 what has been found for European beech forest conditions elsewhere (Dalsgaard et al., 2011). Values of γ_{SM} displayed were obtained from measured emission rates (Pegoraro et al., 2004a; 2004b; Brilli et al., 2007; Fortunati et al., 2008; Bourtsoukidis et al., 2014) and were divided by either (a) the corresponding measurements at well-watered standard conditions or (b) by literature values for the individual plant species. More information on the individual datasets and studies is provided in Table 215 2. Some values such as PWP and nFK are assumed according to the information provided by the authors of the corresponding studies. The figure clearly indicates that most of the studies focused on a specific smaller frame of the entire $SWA\%$ range and only a single value has been measured below the PWP . This smaller range tended to yield a simplified description as for example the dataset of Pegoraro et al. (2004a), which was used by Guenther et al. (2006; 2012)(residual standard error (RSE) = 0.163, $r^2 = 0.65$). Testing different models for the dominating processes, the biological growth curve was found to fit the available datasets best (RSE = 0.06).

220 $\gamma_{SM}(isop, fit, growth) = \exp\left(-\exp((0.056 \pm 0.001) \cdot \exp(1) \cdot (-(2.3 \pm 1.5) - SWA\%) + 1)\right)$ (6a)

$$= \exp\left(-\exp\left(\frac{(0.056 \pm 0.001)}{nFK} \cdot \exp(1) \cdot (-(5.4 \pm 3.5) - (SWC_v - PWP)) + 1\right)\right)$$
 (6b)

Apparently, limited soil water access seems to influence isoprene emissions predominantly by growth stress and less by 225 stomatal opening, although growth stress and stomatal opening share similar features in a plot like Fig. 1 and only the entire $SWA\%$ range allows discrimination between the two. Isoprene may diffuse out of the plant because of its smaller molecular size. Thus, a nearly closed stomata may not protect the plant from the release of isoprene because of enhanced cellular concentrations at reduced stomatal opening (Simpson et al., 1985; Fall et al., 1992).

3.2 Monoterpenes

The situation for monoterpenes (MT) is more complex as different MT isomers display a different behaviour with decreasing $SWA\%$ (and SWC_v , Fig. 2). For example, in the case of European beech (*Fagus sylvatica*) the dominant MT sabinene (Moukhtar 230 et al., 2006) declines drastically with reduced water availability, but limonene to a smaller extend, whereas trans- β -ocimene stays constant within the uncertainty limit (Rombach, 2018). Lüpke et al. (2017a) report declines in α - and β -pinene, limonene and myrcene emissions in response to increasing drought stress on Scots pine (*Pinus sylvestris*), while Δ^3 -carene emissions remained unaffected. An isotopic labeling test displayed a tendency of negatively influenced *de novo* production and contribution with declining SWC_v and thus $SWA\%$, while emission of stored monoterpenes was less affected. This may explain



235 the overall behavior of MT emission and propose the storage pools to determine the total amount of emissions. If so, any
damage to cell walls or other plant structure elements, and extensive drought length will cause a) a significant decline in total
emissions beyond the drought period on the long term, and b) the ability of the plant structure to recover, to form and store
new MT as before. Individual MT structure behaviour however will depend on their detailed production pathway and storage
location within the plant. Ormeno et al. (2007) describe an increase of MT emissions by rosemary (*Rosmarinus officinalis*) at
240 reduced soil water supply under Mediterranean conditions. The individual contribution of different structures even display a
further process to be noted: The relative contribution of α -pinene increased at reduction of SWC_v from 21% to PWP and dropping
thereafter similar to a stress response until cell damage was observed. A secondary contribution increase at very low
 SWC_v values observed for Sweet chestnut (*Castanea sativa*; Lüpke et al., 2017b) may result from changes in very small
emission amounts and appears as large uncertainty range awaiting further investigation. The remaining emission flux below
245 PWP may result from *de novo* production or from different storage locations, which are still functioning properly. Emissions
of sabinene behave in a very similar way to the ones of α -pinene, while the fluxes of myrcene transiently increase around
 PWP . The opposite is true for cineole contribution that drastically declines with reducing SWC_v and displays only at notable
soil water presence. MT emissions of Aleppo pine (*Pinus halepensis*) display a pattern insignificantly influenced by γ_{SM} vs.
250 SWC_v for α -pinene, Δ^3 -carene and linalool, while β -pinene and myrcene tend to increase. Total kermes oak (*Quercus coccifera*)
emissions of MT do not change significantly as well, but the contribution of α -pinene to total MT emissions enhances
continuously even beyond the PWP . Therefore, the effect of individual MT structures depends on production rate as well as
on storage pools and locations, which differ for different plant species. By changing the MT mixture plants may adapt to
different stress conditions for improved defense (more details in section 3.5). However, the total MT emission effect of limited
soil moisture seems to be more general.

255 A representative plot indicating the influence of $SWA\%$ on total MT emissions is shown in Fig. 2. The set-up is identical to Fig.
1 for isoprene, i.e. the different studies included are marked with different symbols and colours. Lighter colours represent
conditions after rewetting if performed as for instance for Scots pine (*Pinus sylvestris*) (Lüpke et al., 2017a). Lighter points
indicate a severe plant structure damage and not entirely recovered plants reaching a lower emission intensity as has been
observed in several studies. Excluding those and assuming a soil water supply above PWP , different fits can be applied to the
260 entire dataset. While all data scatter notably, the best performance is obtained with the hydraulic conductivity approach
(residual standard error (RSE) = 0.02), which is stomata opening controlled. Eventually the biological growth fit (RSE = 0.14)
works appropriately if the smallest values are neglected. However, the three-step approach by Guenther et al. (2006; 2012)
fails (RSE = 0.69) to appropriately describe the observations. Due to different abilities to store MT as commonly denoted as
offline and only temperature driven emissions the lower end of the fit displays a notable variance.

265 $\gamma_{SM}(MT, fit, growth) = (0.22 \pm 0.05) + (0.78 \pm 0.05) \cdot \frac{(1.3 \pm 0.1) \cdot SWA\%}{(33 \pm 3)\% + SWA\%}$ (7a)



$$= (0.22 \pm 0.05) + (0.78 \pm 0.05) \cdot \frac{(1.3 \pm 0.1) \cdot (SWC_v - PWP)}{\frac{(33 \pm 3)\%}{nFK} + (SWC_v - PWP)} \quad (7b)$$

$$\gamma_{SM}(MT, fit, growth) = \exp \left(-\exp \left((0.019 \pm 0.004) \cdot \exp(1) \cdot (-(5.0 \pm 1.2) - SWA\%) + 1 \right) \right) \quad (8a)$$

$$= \exp \left(-\exp \left((0.019 \pm 0.004) \cdot \exp(1) \cdot \left(-(5.0 \pm 1.2) - \frac{(SWC_v - PWP)}{nFK} \right) + 1 \right) \right) \quad (8b)$$

Note, the $SWA\%$ effect is less punctual at a specific $SWA\%$ than in the case of isoprene and the specific slope is soil, i.e. nFK and PWP , dependent. The decline in emission strength gets already larger than 5% by $70 \pm 5\%$ of the accessible $SWA\%$, depending on the fitting model chosen, not at about 6 ± 2 in the case of isoprene as similarly found by Guenther et al. (2012). However, the lower edge of the fitting is different but important especially for arid regions and their corresponding emissions. On average about $22 \pm 5\%$ of the total MT emissions remain unaffected by soil water content (at PWP).

3.3 Sesquiterpenes

Based on the molecular properties such as saturation vapour pressure (Seinfeld and Pandis, 2016), water solubility (Sander, 2015), and capability to be stored (Kosina et al., 2012), the effect of $SWA\%$ on the emissions of sesquiterpenes (SQT, $C_{15}H_{24}$) (Duhl et al., 2008) behaves the same way as seen for MT (Fig. 3), i.e. emissions are predominantly affected by plant hydraulic conductivity ($RSE = 0.153$), which is controlled by stomatal opening. Applying the same approach as done for monoterpenes above, yields the following results for the soil moisture effect on total sesquiterpene emission rates $\gamma_{SM}(SQT)$:

$$\gamma_{SM}(SQT, fit, hyd.) = (0.22 \pm 0.04) + (0.78 \pm 0.04) \cdot \frac{(1.75 \pm 0.5) \cdot SWA\%}{(81 \pm 57)\% + SWA\%} \quad (9a)$$

$$= (0.22 \pm 0.05) + (0.78 \pm 0.05) \cdot \frac{(1.75 \pm 0.5) \cdot (SWC_v - PWP)}{\frac{(81 \pm 57)\%}{nFK} + (SWC_v - PWP)} \quad (9b)$$

The onset of emission reduction with decreasing $SWA\%$ sets in even earlier compared to MTs (Rombach, 2018), as indicated by the different slopes in Fig. 3 and in Eqs. (9a and 9b). However, individual structures reveal a large scattering at lower $SWA\%$ and thus SWC_v values (<10%) that is supposed to result from plant defensive strategies/mechanisms and perhaps from damage to cell walls and membranes.

3.4 Potential additional effects near the wilting point for terpenes

For some plant species e.g. *Cistus albidus* and rosemary (*Rosmarinus officinalis*), the effects of limited access to soil water on MT and SQT emission fluxes reveal a second maximum other than the one at $\gamma_{SM} = 1$, appearing near the PWP (Figs. 4, S3-S8). Highly temperature- and drought stress adapted species with the ability of to produce large amounts of terpenoids (e.g.



290 *Cistus ladanifer* (Haberstroh et al., 2018) and *Rosmarinus officinalis* (Ormeno et al., 2007)) display a second maximum close to *PWP* not only for some of the MT (*Cistus ladanifer*: d-limonene, myrcene and trans- β -ocimene (Haberstroh et al., 2018); *Rosmarinus off.*: α -pinene and β -myrcene (Ormeno et al., 2007)) but also for some of the SQT (*Cistus ladanifer*: α -cubebene, α -farnesene, ent-16-kaurene and β -chamigrene (Haberstroh et al., 2018); *Rosmarinus off.*: Δ -cardinene and α -zingiberene (Ormeno et al., 2007), Fig. 4) and even the sum of all. This is apparent for instance in the studies of Ormeno et al. (2007) and
295 Haberstroh et al. (2018) of a broader range of plant species. As can be seen in Figs. S3-S8 (supporting online information), there is a statistically significant difference between individual chemical structures for different plant species, indicating a specifically adopted plant species. If those plots are investigated in more detail it is apparent that for example the monoterpene α -pinene increases with decreasing *SWA%* for *Rosmarinus officinalis* (S6) and *Quercus coccifera* (S5), but persists for *Pinus halepensis* (S4) (Ormeno et al., 2007). The emission of the monoterpene β -pinene is declining for *Cistus albidus* (S3), stays
300 put for *Rosmarinus officinalis* (S6) and enhances for *Pinus halepensis* and *Quercus coccifera*. Similar observations can be made for SQT emissions with *SM* values near the *PWP*: Δ -cadinene emissions increase with decreasing *SM*, while α -zingiberene emission decline for *Rosmarinus officinalis*. Haberstroh et al. (2018) monitored decreasing emission fluxes for all the individual chemical SQT structures for *Cistus ladanifer* and *Quercus robur* in a very narrow *SM* range (*SWA%* = ca. 0-6 %). This is opposite to the behaviour of *Cistus albidus* (Ormeno et al., 2007). Δ -germacrene emissions tend to increase near the *PWP* for
305 *Cistus albidus*, *Quercus coccifera* and *Rosmarinus officinalis* (Figs. S3, S5 and S6).

The enhanced emitted chemical species are known to possess a substantially higher reactivity with respect to ozone, which is usually elevated at drier conditions on longer time scales because of enhanced production rates and accumulation (see section 3.7). For example α -pinene possesses an O_3 reaction rate constant (k_{O_3}) of $8.66 \times 10^{-17} \text{ cm}^{-3} \text{ molecule}^{-1} \text{ s}^{-1}$, compared to the ones of β -pinene and Δ^3 -carene of 1.5×10^{-17} and $3.7 \times 10^{-17} \text{ cm}^3 \text{ molecule}^{-1} \text{ h}^{-1}$, respectively (Atkinson et al., 1990). With respect to
310 the OH reaction, β -pinene reacts fastest ($k_{OH} = 7.89 \times 10^{-11} \text{ cm}^3 \text{ molecule}^{-1} \text{ h}^{-1}$), followed by α -pinene and Δ^3 -carene with corresponding rate constant k_{OH} of 5.37×10^{-11} and $0.88 \times 10^{-11} \text{ cm}^3 \text{ molecule}^{-1} \text{ h}^{-1}$, (Atkinson and Arey, 2003). This can be extended for other monoterpenes if more data especially on d-limonene, terpinolene and other very reactive MTs would be available. However, the number of data for individual species is quite limited and depends on different plant ages, which does not allow deriving a trustworthy equation at this stage. Sometimes the number of data points is equal to the number of
315 parameters to constrain. The situation looks similar for SM effects on SQT emission rates. Consider e.g. the bottom plot for SQT in Fig. 4, displaying allo-aromadendrene, Δ -germacrene, Δ -cadinene and α -zingiberene. Reaction rate constants k_{O_3} with respect to ozone are 6.5×10^{-16} , unknown, 3.2×10^{-16} and unknown, respectively. The corresponding k_{OH} for OH reactions are $1.5 \times 10^{-10} \text{ cm}^3 \text{ molecule}^{-1} \text{ h}^{-1}$ for aromadendrene, with the further ones not accessible based on experiments. However, structure-activity relationships such as EPI Suite (2018), indicate constants of ca $10^{-10} \text{ cm}^3 \text{ molecule}^{-1} \text{ h}^{-1}$. Thus, we assume this
320 secondary maximum to occur as detoxification and defensive strategy of the plants (Kaurinovic et al., 2010; Höferl et al., 2015). Because of notable variations in measurements this effect is not significant for all the Mediterranean species, but for



the *Cistus ladanifer* and *Rosmarinus officinalis* measurements. To incorporate this feature near the PWP exemplarily, which tends to be linked to higher ozone concentrations, this secondary maximum can be taken into account using a Gamma function term added to the hydraulic conductivity curve (RSE = 0.147) in Eqs. 9a and 9b:

$$325 \quad \gamma_{SM}(SQT, fit, hyd.)^* = (0.22 \pm 0.04) + (0.78 \pm 0.04) \cdot \frac{(1.75 \pm 0.5) \cdot SWA\%}{(81 \pm 57)\% + SWA\%} \\ + a \cdot (SWA\% + b)^c \cdot \exp(-d \cdot (SWA\% + b)) \quad (9a)$$

$$\gamma_{SM}(SQT, fit, hyd.)^* = (0.22 \pm 0.04) + (0.78 \pm 0.04) \cdot \frac{(1.75 \pm 0.5) \cdot (SWC_v - PWP)}{(81 \pm 57)\% + (SWC_v - PWP)} \\ + a \cdot \left(\frac{SWC_v - PWP}{nFK} + b \right)^c \cdot \exp \left(-d \cdot \left(\frac{SWC_v - PWP}{nFK} + b \right) \right) \quad (9b)$$

330 *a, b, c* and *d* state parameters for the individual response of plant species to severe drought stress Gamma function) and they need to be adapted to the exact plant or ecosystems response studied on the local scale. An example is shown by the green line in Fig. 3 (applied parameters in here for *Cistus ladanifer* and *Rosmarinus officinalis*: *a* = 0.4, *b* = 1.57, *c* = 0.6, *d* = 1). It is of interest that different structures seem to behave differently according to their historical stress adaptation as presented by Fortunati et al. (2008) and Lüpke et al. (2016). On the contrary to the hydraulic conductivity related description, the stepwise approach (Guenther et al., 2006) fails in reproducing the declining pattern accurately (RSE = 0.895).

335

3.5 Further BVOC emission rates

In addition to isoprene, MT and SQT, other VOCs are released by plants in notable amounts, but for which the impact of soil moisture is even less studied. Because of the huge number of different oxidized species and related publications including those within the parameterization would extend this study largely. A snapshot of individual correlation coefficients of different 340 compound groups and species can be seen in Figure S1. A non-negligible role of those larger VOCs seems plausible, either via formation pathway or oxidation processes within the plant. Those species supply further molecules that can buffer oxidative stresses onto the plants internal processes. Additionally, they have substantial implications on especially the OH reactivity (Atkinson et al., 1990; Atkinson and Arey, 2003; Neeb, 2000; Münz, 2010; Seinfeld and Pandis, 2016, US EPA, 2018). Overall, there is a tendency for an increased total BVOC emission under drought stressed conditions, but there is a large scatter of 345 individual species reaction. However, the implications for OH reactivity and thus atmospheric chemistry are of relevance as this parameter describes the plants ability to still counteract oxidative damages by BVOC emissions.



3.6 Effects on reactivity

As chemical oxidation and ROS cause substantial damage to plants (Loreto and Velikova, 2001; Oikeawa et al., 2013) especially at stressed conditions such as at warm and dry conditions, any strategy of plants to counteract or detoxify will be beneficial for survival and plant competition. An indication for this may be seen in the local emission increase of SQT near PWP for some plant species. Saunier et al. (2017) found a stable ratio of catabolic to anabolic BVOC emissions, i.e. emission fluxes related to oxidation stress and to non-oxidative stress production, respectively, during recurring drought periods for downy oak (*Quercus pubescens*) at Mediterranean conditions. This is different for different plant types and their adaptation to stress conditions (Niinemets, 2010a; 2010b), i.e. the need to compensate oxidative stress for survival. Looking at the pattern of absolute and relative MT and SQT emissions with declining SWA% values, it becomes obvious that more reactive structures tend to increase until plant cell damages occur (Ormeno et al., 2007; Bourtsoukidis et al., 2012; Nölscher et al., 2016). Especially SQT emissions displaying this transient peak around PWP cause a remarkable change. For example reducing the SWC_v for European beech by approximately 3 vol% close to PWP increases the total emission of SQTs by 170%. The individual SQT species, however, show different patterns (Table 2). While emission of junipene declines (-50%), the one of longifolene stays constant within the uncertainty limits and the corresponding fluxes of isolongifolene, α -bergamotene and α -farnesene increase drastically (+50%, +500% and +700%). Other VOCs analyzed (total: 81 VOCs; Rombach, 2018) operate in various ways: sabinene emission nearly vanishes at PWP. On the contrary, emission of α -terpineol increased. Overall, the total emissions of VOCs and C increased tentatively (Fig. 5). This caused total OH reactivity and especially ozone reactivity to tentatively enhance (OH: $+39^{+88}_{-46}\%$ and O₃: $+131^{+265}_{-104}\%$) at a SWC_v change of approximately 3 vol%. In this way the total amount, the changing composition and reactivity provide a tool for plants in this example for European beech to counteract oxidative stress and damages. The median change in OH reactivity corresponds nicely to the increase in total carbon emitted, as most organic species react with OH. However, the change in ozone reactivity is primarily related to the changes in individual SQT emissions. The large uncertainty in this context results from partially unknown reaction rate constants estimated either from similarity or from structure activity relationships (SAR) (Neeb, 2000; McGillen et al., 2011). Since the storage pools especially of larger terpenes will be depleted with prolonged duration of drought, this effect will weaken over time.

3.7 Application to atmospheric conditions: Ambient SWC_v and its effect on emission rates at the reference site

In order to test the impact of the described effects of SWA% and thus SWC_v on isoprenoid emissions we apply the following emission flux parameterizations for isoprenoids from European beech and silver fir, which were quantified in earlier studies in this region excluding the SWA% effect (Moukhtar et al., 2005; 2006; Šimpraga et al., 2011; Bonn et al., 2017):

$$E_{isop}(Fs) = 0 \text{ } \mu\text{g g(dw)}^{-1} \text{ h}^{-1} * C_T * C_L \quad (10a)$$

$$E_{MT}(Fs) = 43.5 \text{ } \mu\text{g g(dw)}^{-1} \text{ h}^{-1} * C_T * C_L \quad (10b)$$



$$E_{SQT}(Fs) = 0.04 \text{ } \mu\text{g g(dw)}^{-1} \text{ h}^{-1} * \exp(0.11 \text{ } ^\circ\text{C}^{-1} * (T_L - 30^\circ\text{C})) \quad (10\text{c})$$

$$E_{isop}(Aa) = 0.038 \text{ } \mu\text{g g(dw)}^{-1} \text{ h}^{-1} * C_T * C_L \quad (10\text{d})$$

380 $E_{MT}(Aa) = 28.8 \text{ } \mu\text{g g(dw)}^{-1} \text{ h}^{-1} * (0.71 * \exp(0.14 \text{ } ^\circ\text{C}^{-1} * (T_L - 30^\circ\text{C})) + 0.29 * C_T * C_L) \quad (10\text{e})$

$$E_{SQT}(Aa) = 0.13 \text{ } \mu\text{g g(dw)}^{-1} \text{ h}^{-1} * \exp(0.04 \text{ } ^\circ\text{C}^{-1} * (T_L - 30^\circ\text{C})). \quad (10\text{f})$$

SM effects on specific emission rates have been calculated by including and excluding the individual γ_{SM} factors as multiplicand on the results. In Eqs. 10a-10f C_T and C_L abbreviate the temperature and light scaling factors of Guenther et al. (1995), as well as T_L the temperature of the needle or leaf surface in $^\circ\text{C}$.

385 The base effect of soil water on isoprenoid emission rates can be exemplarily shown assuming a temperature of 30 $^\circ\text{C}$, i.e. standard conditions (see Fig. S2 in supporting online information). The available soil water for a plant has different impacts at distinct SWA% values. At SWA% (i.e. SWC_v (Freiamt) = 20%) of 35% isoprene emission rates display no decline, while the corresponding ones of MT and SQT reduce by 15 and 25%, respectively. Assuming an SWA% of 10% (SWC_v = 10% with a PWP of 4.8% at Freiamt), isoprene, MT and SQT emission rates represent only 95, 50 and 40% of the standard rates. Therefore, 390 the amount of soil water has strongest effects on the larger terpenes shrinking with molecular size. Isoprene emissions will stay unaffected longer than MT and will keep ozone production high if isoprene is the dominant class of isoprenoids released by the ecosystems in the nearby region. Depending on the tree specific emission – i.e. on- and offline including temperature effects – different locations of emission optima or maxima are found (Fig. 6). The predominantly *de novo* emitting European beech will emit highest close to 30 $^\circ\text{C}$, while the maxima of silver fir emission rates are shifted to larger temperatures. Similarly 395 the effects of changing SM will occur at the very same temperatures.

The overall impact of variable SM pattern on isoprenoid emissions was investigated using an exemplary SWC_v data at five different depths. Those measurements were located within the reference stand of a European beech (*Fagus sylvestris*, *Fs*) and silver fir (*Abies alba*, *Aa*) of the BuTaKli project in Freiamt within the Black Forest (Southwestern Germany) region (Magh et al., 2018). In general, the uppermost layer is drying out fastest especially during summertime, while lower layers, i.e. below 400 30 cm, retain a higher SWC_v for a longer time period. This implies different effects on the tree species with different rooting depths and thus access to soil water. Regarding the effect of SM on isoprenoid emissions - i.e. the g factor - the g_{SM} values for one vegetation period (during 2016) are shown in Fig. 7. Individual plots represent the SWC_v emission effects of different compounds or compound classes and different colours illustrate the SWC_v based values for three different depths. Apparently 405 during summertime, when the evapotranspiration flux and the emission rates are highest due to elevated temperatures and radiation intensity, the effect is most intense. During the rather well watered summer 2016 $\gamma_{SM}(isop)$ caused reduction by almost 40% for more shallow rooting species and by 20 to 30% for trees with access to deeper soil layers (60 cm in depth).



$\gamma_{SM}(MT)$ declined to nearly 55% on average with short time access to more water for deeper roots and $\gamma_{SM}(SQT)$ to nearly 60% of emission rates.

During 2017 with an improved roof cover, the differences between different soil depths became more obvious, and they exceed
410 effect changed by 10% or more between 40 and 60 cm in depth (not shown, (Magh et al., in prep). Those effects are estimated to intensify remarkably during extensive drought periods such as occurred in summer 2018, of which no dataset is available. This is going to take down most of the BVOC emission rates with progressing drought period time, depending on the tree species rooting depth and soil water access. Therefore, the total sum of isoprenoid emissions of a specific forest ecosystem will be reflected by the individual contribution of tree species and its specific emission pattern, and the sum of SM affects the
415 drought sensitivity of the ecosystem.

4 Conclusions

In this study we derived three sets of parameterizations for the influence of soil moisture on isoprenoid emission rates. Those depend on the details of soil characteristics, plant properties of on- and offline production of isoprenoids and potential defensive plant feedback mechanisms on oxidative stress. The effect on isoprene emissions acts similar as a small molecule able to
420 penetrate the plant surface acting like a biological growth stress. While the cuticula provides some minor resistance it cannot hinder isoprene from penetration at nearly closed stomata. Thus, the present description allows minor isoprene emissions below the *PWP*. The influence of soil water access on larger isoprenoid emission occurs on a notably larger range of *SWA%* as a function of stomata opening (hydraulic conductivity pattern). Depending on the specific tree species some molecular structures of terpenes e.g. the more reactive ones like α -pinene and β -myrcene (Haberstroh et al., 2018; Ormeno et al., 2007) and α -
425 farnesene (Duhl et al., 2008; Haberstroh et al., 2018) display an elevated relative terpene flux contribution at lower soil moisture (Figs. S3-S8), indicating a defensive strategy of plants against oxidative stress at lower soil water concentrations, thus warmer conditions and in total critical for the plants survival. This is plant species dependent and can be incorporated by a secondary maximum close to the permanent wilting point. The named *SWA%* impact on isoprenoid emission rates is expected to induce several feedback processes in the atmosphere and climate system including local tropospheric ozone production and sink
430 (Seinfeld and Pandis, 2016), new particle formation (Bonn et al., 2014; Bonn 2014) and growth as well as cloud condensation nuclei (Bonn 2014; Seinfeld and Pandis, 2016). With these findings we conclude that more studies on available soil water dependence of emissions of higher terpenes, oxygenates and follow-up processes, are essentially needed for different environments to realistically describe the natural feedback processes of forests and ecosystems in changing climate conditions and the anthropogenic impact on these. Because of that, the *SWA%* concepts described should definitely be included in
435 corresponding global atmospheric chemistry transport models in order to cover not only plant response to the expected increase in drought periods but to future development of biosphere-atmosphere processes, resulting in adaptation or extinction in a changing climate.



Supplementary Materials: Supplementary material is available as an additional file.

Author Contributions: B.B. was responsible for the methodology, analysis and writing. R.-K.M. conducted the SWC_v measurements and
440 soil texture analysis, contributed to the data analysis and parameterization approach and was responsible for the soil water concepts. The formal analysis of *Fagus sylvatica* BVOC emissions and water potential measurements at the campus field site was done by J.R. J.K. contributed by conceptualization of the *Fagus sylvatica* campus field site experiment, discussion about accurate plant physiology process description as well as review and editing.

Funding: This research was funded by German Waldklimafond project BuTaKli, no. 100261371.

445 **Acknowledgments:** Funding within the German Waldklimafond project BuTaKli (no. 100261371) is kindly acknowledged. Highly acknowledged is the supply of SWC_v data for Campus Flugplatz soil texture by Angelika Küberts and Simon Haberstrohs support with further information and data on the Haberstroh et al. (2018) measurements. Thanks go to the supporting staff and colleagues at Freiburg University and to all partners within the BuTaKli project for their nice support and exchange of information and data, too. We thank the R Development Core Team for providing version 3.5.1 with its individual tool packages (R Core Team, 2017), which were used for conducting
450 this study.

Conflicts of Interest: The authors declare no conflict of interest.

References

Atkinson, R., and Arey, J.: Gas-phase tropospheric chemistry of biogenic volatile organic compounds: a review. *Atmos. Environ.*, 37, S197-S219, doi: 10.1016/S1352-2310(03)00391-1, 2003.

455 Atkinson, R., Hasegawa, D., and Aschmann, S.M.: Rate constants for the gas-phase reactions of O_3 with a series of monoterpenes and related compounds at 296 ± 2 K. *Int. J. Chem. Kinet.*, 22, 871-887, 1990.

Blume, H.-P., Brümmer, G. W., Horn, R., Kandeler, E., Kögel-Knabner, I., Kretzschmar, R., Stahr, K., Wilke, B.-M., Thiele-Bruhn, S., and Welp, G.: Scheffer/Schachtschabel: Lehrbuch der Bodenkunde. Spektrum Akad. Verlag. p.570, Heidelberg, 2010.

Bonn, B., Bourtsoukidis, E., Sun, T. S., Bingemer, H., Rondo, L., Javed, U., Li, J., Axinte, R., Li, X., Brauers, T., Sonderfeld, H., Koppmann, 460 R., Sogachev, A., Jacobi, S., and Spracklen, D. V.: The link between atmospheric radicals and newly formed particles at a spruce forest site in Germany. *Atmos. Chem. Phys.*, 14, 10823–10843, doi: 10.5194/acp-14-10823-2014, 2014.

Bonn, B.: Biogene Terpenemissionen und sekundäre Aerosolpartikelbildung: Ein Weg von Nadelwäldern Klimarückkopplungsprozesse zu steuern. Prof. thesis, J. W. Goethe Universität, p.336, Frankfurt/Main, 2014.

Bonn, B., Kreuzwieser, J., Sander, F., Yousefpour, R., Baggio, T., and Adewale, O.: The uncertain role of biogenic VOC for boundary-layer 465 ozone concentration: Example investigation of emissions from two forest types with a box model. *Climate*, 5, 78-98, doi:10.3390/cli5040078, 2017.

Bonn, B., Sperlich, D., Schindler, D., Magh, R.-K., Grote, R., Rehschuh, S., Dannenmann, M., Kreuzwieser, J., Rennenberg, H., Trautmann, R., and Yousefpour, R.: Counteracting climate change: The impacts of intermixing European beech forests with silver fir on the radiation regime in Southwestern Germany. *Atmos. Environ.*, in prep.



470 Bourtsoukidis, E., Bonn, B., Dittmann, A., Hakola, H., Hellén, H., and Jacobi, S.: Ozone stress as a driving force of sesquiterpene emissions: A suggested parameterisation. *Biogeosciences*, 9, 4337–4352, doi: 10.5194/bg-9-4337-2012, 2012.

Bourtsoukidis, E., Kawaletz, H., Radacki, D., Schütz, S., Hakola, H., Hellén, H., Noe, S., Mölder, I., Ammer, C., and Bonn, B.: Impact of flooding and drought conditions on the emission of volatile organic compounds of *Quercus robur* and *Prunus serotina*. *Trees - Struct. Funct.*, 28, 193–204, doi: 10.1007/s00468-013-0942-5, 2014.

475 Brilli, F., Barta, C., Fortunati, A., Lerdau, M., Loreto, F., and Centritto, M.: Response of isoprene emission and carbon metabolism to drought in white poplar (*Populus alba*) saplings. *New Phytol.*, 175, 244–254, doi: 10.1111/j.1469-8137.2007.02094.x, 2007.

Chen, F., and Dudhia, J.: Coupling an advanced land surface-hydrology model with the Penn State-NCAR MM5 modeling system. Part 1: Model implementation and sensitivity. *Mon. Weather Rev.* 129, 569–585, doi: 10.1175/1520-0493(2001)129<0569:CAALSH>2.0.CO;2, 2001.

480 Dalsgaard, L., Mikkelsen, T. N., and Bastrup-Birk, A.: Sap flow for beech (*Fagus sylvatica* L.) in a natural and a managed forest - Effect of spatial heterogeneity. *J. Plant Ecol.*, 4, 23–35, doi: 10.1093/jpe/rtq037, 2011.

Duhl, T. R., Helmig, D., and Guenther, A.: Sesquiterpene emissions from vegetation: A review. *Biogeosciences*, 5, 761–777, doi: 10.5194/bg-5-761-2008, 2008.

Fall, R., and Monson, R. K.: Isoprene emission rate and intercellular isoprene concentration as influenced by stomatal distribution and 485 conductance. *Plant Physiol.*, 100, 987–992, doi: 10.1104/pp.100.2.987, 1992.

Fortunati, A., Barta, C., Brilli, F., Centritto, M., Zimmer, I., Schnitzler, J. P., and Loreto, F.: Isoprene emission is not temperature-dependent during and after severe drought-stress: A physiological and biochemical analysis. *Plant J.*, 55, 687–697, doi: 0.1111/j.1365-313X.2008.03538.x, 2008.

490 Genard-Zielinski, A. C., Boissard, C., Ormeño, E., Lathière, J., Reiter, I. M., Wortham, H., Orts, J. P., Temime-Roussel, B., Guenet, B., Bartsch, S., Gauquelin, T., and Fernandez, C.: Seasonal variations of *Quercus pubescens* isoprene emissions from an in natura forest under drought stress and sensitivity to future climate change in the Mediterranean area. *Biogeosciences*, 15, 4711–4730, doi: 10.5194/bg-15-4711-2018, 2018.

Gessler, A., Keitel, C., Kreuzwieser, J., Matyssek, R., Seiler, W., and Rennenberg, H.: Potential risks for European beech (*Fagus sylvatica* L.) in a changing climate. *Trees - Struct. Funct.*, 21, 1–11, doi: 10.1007/s00468-006-0107-x, 2007.

495 Ghirardo, A., Koch, K., Taipale, R., Zimmer, I., Schnitzler, J. P., and Rinne, J.: Determination of de novo and pool emissions of terpenes from four common boreal/alpine trees by $^{13}\text{CO}_2$ labelling and PTR-MS analysis. *Plant, Cell Environ.*, 33, 781–792, doi: 10.1111/j.1365-3040.2009.02104.x, 2010.

Goldstein, A. H., and Galbally, I. E.: Known and unexplored organic constituents in the Earth's atmosphere. *Environ. Sci. Technol.*, 41, 1514–1521, doi: 10.1021/es072476p, 2007.

500 Guenther, A., Hewitt, C. N., Erickson, D., Fall, R., Geron, C., Graedel, T., Harley, P., Klinger, L., Lerdau, M., McKay, W. A., Pierces, T., Scholes, B., Steinbrecher, R., Tallamraju, R., Taylor, J., and Zimmerman, P.: A global model of natural volatile organic compound emissions. *J. Geophys. Res.*, 100, 8873–8892, doi: 10.1029/94JD02950, 1995.

Guenther, A., Karl, T., Harley, P., Wiedinmyer, C., Palmer, P. I., and Geron, C.: Estimates of global terrestrial isoprene emissions using 505 MEGAN (Model of Emissions of Gases and Aerosols from Nature). *Atmos. Chem. Phys.*, 6, 3181–3210, doi: 10.5194/acp-6-3181-2006, 2006.



Guenther, A. B., Jiang, X., Heald, C. L., Sakulyanontvittaya, T., Duhl, T., Emmons, L. K., and Wang, X.: The Model of Emissions of Gases and Aerosols from Nature Version 2.1 (MEGAN2.1): An extended and updated framework for modeling biogenic emissions. *Geosci. Model Dev.*, 5, 1471–1492, doi: 10.5194/gmd-5-1471-2012, 2012.

Haberstroh, S., Kreuzwieser, J., Lobo-do-Vale, R., Caldeira, M. C., Dubbert, M., and Werner, C.: Terpenoid emissions of two Mediterranean woody species in response to drought stress. *Front Plant Sci.*, 9, 1–17, 1071, doi: 10.3389/fpls.2018.01071, 2018.

Hansen, U., and Seufert, G.: Terpenoid emission from *Citrus sinensis* (L.) OSBECK under drought stress. *Phys. Chem. Earth, Part B Hydrol. Ocean. Atmos.*, 42, 681–687, doi: 10.1016/S1464-1909(99)00065-9, 1999.

Höferl, M., Stoilova, I., Wanner, J., Schmidt, E., Jirovetz, L., Trifonova, D., Stanchev, V., and Krastanov, A.: Composition and Comprehensive Antioxidant Activity of Ginger (*Zingiber officinale*) Essential Oil from Ecuador. *Nat. Prod. Commun.*, 10, 1085–1090, ISSN: 1934-578X, 1555-9475, 2015.

Holopainen, J. K., Kivimäenpää, M., and Nizkorodov, S. A.: Plant-derived secondary organic material in the air and ecosystems. *Trends Plant Sci.*, 22, 744–753, doi: 10.1016/j.tplants.2017.07.004, 2017.

IPCC. IPCC 2013, Stocker, T.F., Qin, D., Plattner, G.-K., Tignor, M., Allen, S.K., Boschung, J., Nauels, A., Xia, Y., Bex, V., Midgley, P. M. (eds.), Cambridge University Press: Cambridge, New York, ISBN: 978-1-107-66182-0, 2013.

Kändler, G., and Cullman, D.: Bundeswaldinventur III: Regionale Auswertung der Bundeswaldinventur Wuchsgebiet Schwarzwald, 2016.

Kaurinovic B., Vlajisljevic, S., Popovic, M., Vastag, D., and Djurendic-Brenesel, M.: Antioxidant properties of *Marrubium peregrinum* L. (*Lamiaceae*) essential oil. *Molecules*, 15, 5943–5955, ISSN: 1420-3049, 2010.

Keuler, K., Radtke, K., Kotlarski, S., and Lüthi, D.: Regional climate change over Europe in COSMO-CLM: Influence of emission scenario and driving global model. *Meteorol. Z.*, 25, 121–136, doi: 10.1127/metz/2016/0662, 2016.

Kreienkamp, F., Paxian, A., Früh, B., Lorenz, P., and Matulla, C.: Evaluation of the empirical–statistical downscaling method EPISODES. *Clim. Dynam.*, ISSN: 1432-0894, pp.36, doi: 10.1007/s00382-018-4276-2, 2018.

Kleiber, A., Duan, Q., Jansen, K., Junker, L. V., Kammerer, B., Rennenberg, H., Ensminger, I., Gessler, A., Kreuzwieser, J.: Drought effects on root and needle terpenoid content of a coastal and an interior douglas fir provenance. *Tree Physiol.*, 37, 1648–1658, doi: 10.1093/treephys/tpx113, 2017.

Kosina, J., Dewulf, J., Viden, I., Pokorska, O., and Van Langenhove, H.: Dynamic capillary diffusion system for monoterpene and sesquiterpene calibration: Quantitative measurement and determination of physical properties. *Int. J. Environ. An. Ch.*, 93, 1–13, doi: 10.1080/03067319.2012.656621, 2012.

Lappalainen, H. K., Sevanto, S., Bäck, J., Ruuskanen, T. M., Kolari, P., Taipale, R., Rinne, J., Kulmala, M., and Hari, P.: Day-time concentrations of biogenic volatile organic compounds in a boreal forest canopy and their relation to environmental and biological factors. *Atmos. Chem. Phys.*, 9, 5447–5459, doi: 10.5194/acp-9-5447-2009, 2009.

Laothawornkitkul, J., Taylor, J. E., Paul, N. D., and Hewitt, C. N.: Biogenic volatile organic compounds in the Earth system: Tansley review. *New Phytol.*, 183, 27–51, doi: 10.1111/j.1469-8137.2009.02859.x, 2009.

Lavoir, A. V., Staudt, M., Schnitzler, J. P., Landais, D., Massol, F., Rocheteau, A., Rodriguez, R., Zimmer, I., and Rambal, S.: Drought reduced monoterpene emissions from the evergreen Mediterranean oak *Quercus ilex*: Results from a throughfall displacement experiment. *Biogeosciences*, 6, 1167–1180, doi: 10.5194/bg-6-1167-2009, 2009.

Leij, F. J., Alves, W. J., van Genuchten, M. T., and Williams, J. R.: Unsaturated Soil Hydraulic Database, UNSODA 1.0 User's Manual, 1996.



Loreto, F., and Velikova, V.: Isoprene produced by leaves protects the photosynthetic apparatus against ozone damage, quenches ozone products, and reduces lipid peroxidation of cellular membranes. *Plant Physiol.*, 127, 1781–1787, doi:10.1104/pp.010497, 2001.

545 Lüpke, M., Leuchner, A., Steinbrecher, R., and Menzel, A.: Impact of summer drought on isoprenoid emissions and carbon sink of three Scots pine provenances. *Tree Physiol.*, 36, 1382–1399, doi:10.1093/treephys/tpw066, 2016.

Lüpke, M., Leuchner, M., Steinbrecher, R., Menzel, A.: Quantification of monoterpane emission sources of a conifer species in response to experimental drought. *AoB Plants*, X, plx045, doi: 10.1093/aobpla/plx045, 2017.

550 Lüpke, M., Steinbrecher, R., Leuchner, M., and Menzel, A.: The Tree Drought Emission MONitor (Tree DEMON), an innovative system for assessing biogenic volatile organic compounds emission from plants. *Plant Methods*, 13, 14, doi: 10.1186/s13007-017-0166-6, 2017.

Magh, R.-K., Yang, F., Rehschuh, S., Burger, M., Dannenmann, M., Pena, R., Burzlaff, T., Ivanković, M., and Rennenberg, H.: Nitrogen nutrition of European beech is maintained at sufficient water supply in mixed beech-fir stands. *Forests*, 9, 733, doi:10.3390/f9120733, 2018.

555 Magh, R.-K., Eiferle, C., Dannenmann, M., Dubbert, M., and Rennenberg, H.: Water use strategies of beech and silver fir in a temperate forest after prolonged drought. *in prep.*

Manninen, A. M., Vuorinen, M., and Holopainen, J. K.: Variation in growth, chemical defense, and herbivore resistance in Scots pine provenances. *J. Chem. Ecol.*, 24, 1315–1331, doi: 10.1023/A:1021222731991, 1998.

560 McGillen, M. R., Ghalaieny, M., and Percival, C. J.: Determination of gas-phase ozonolysis rate coefficients of C8-14 terminal alkenes at elevated temperatures using the relative rate method. *Phys. Chem. Chem. Phys.*, 13, 10965–10969, doi: 10.1039/c0cp02643c, 2011.

Mogensen, D., Gierens, R., Crowley, J. N., Keronen, P., Smolander, S., Sogachev, A., Nölscher, A. C., Zhou, L., Kulmala, M., Tang, M. J., Williams, J., and Boy, M.: Simulations of Atmospheric OH, O₃ and NO₃ reactivities within and above the Boreal Forest. *Atmos. Chem. Phys.*, 15, 3909–3932, doi: 10.5194/acp-15-3909-2015, 2015.

565 Moukhtar, S., Bessagnet, B., Rouil, L., and Simon, V.: Monoterpene emissions from beech (*Fagus sylvatica*) in a French forest and impact on secondary pollutants formation at regional scale. *Atmos. Environ.*, 39, 3535–3547, doi: 10.1016/j.atmosenv.2005.02.031, 2005.

Moukhtar, S., Couret, C., Rouil, L., and Simon, V.: Biogenic volatile organic compounds (BVOCs) emissions from *Abies alba* in a French forest. *Sci. Total Environ.*, 354, 232–245, doi: doi:10.1016/j.scitotenv.2005.01.044, 2006.

Neeb, P.: Structure-reactivity based estimation of the rate constants for hydroxyl radical reactions with hydrocarbons. *J. Atmos. Chem.*, 35, 295–315, doi: 10.1023/A:1006278410328, 2000.

570 Niinemets, Ü.: Mild versus severe stress and BVOCs: Thresholds, priming and consequences. *Trends Plant Sci.*, 15, 145–153, doi: 10.1016/j.tplants.2009.11.008, 2010a.

Niinemets, Ü.: Responses of forest trees to single and multiple environmental stresses from seedlings to mature plants: Past stress history, stress interactions, tolerance and acclimation. *Forest Ecol. Manage.*, 260, 1623–1639, doi: 10.1016/j.foreco.2010.07.054, 2010b.

575 Niinemets, Ü., Fares, S., Harley, P., and Jardine, K. J.: Bidirectional exchange of biogenic volatiles with vegetation: Emission sources, reactions, breakdown and deposition. *Plant Cell Environ.*, 37, 1790–1809, doi: 10.1111/pce.12322, 2014.

Nölscher, A. C., Butler, T., Auld, J., Veres, P., Muñoz, A., Taraborrelli, D., Vereecken, L., Lelieveld, J., and Williams, J.: Using total OH reactivity to assess isoprene photooxidation via measurement and model. *Atmos. Environ.*, 89, 453–463, doi: 10.1016/j.atmosenv.2014.02.024., 2014

Nölscher, A. C., Yañez-Serrano, A. M., Wolff, S., De Araujo, A. C., Lavrič, J. V., Kesselmeier, J., and Williams, J.: Unexpected seasonality in quantity and composition of Amazon rainforest air reactivity. *Nat. Commun.*, 7, 10383, p.11, doi: 10.1038/ncomms10383, 2016.



Oikawa, P. Y. and Lerdau, M. T.: Catabolism of volatile organic compounds influences plant survival. *Trends Plant Sci.*, 18, 695–703, doi: 10.1016/j.tplants.2013.08.011, 2013.

Ormeño, E., Mévy, J.P., Vila, B., Bousquet-Mélou, A., Greff, S., Bonin, G., and Fernandez, C.: Water deficit stress induces different monoterpane and sesquiterpene emission changes in Mediterranean species. Relationship between terpene emissions and plant water potential. *Chemosphere*, 67, 276–284, doi: 10.1016/j.chemosphere.2006.10.029, 2007.

585 Pegoraro, E., Rey, A., Bobich, E. G., Barron-Gafford, G., Grieve, K. A., Malhi, Y., and Murthy, R.: Effect of elevated CO₂ concentration and vapour pressure deficit on isoprene emission from leaves of *populus deltoides* during drought. *Funct. Plant Biol.*, 31, 1137–1147, doi: 10.1071/FP04142, 2004a.

Pegoraro, E., Rey, A., Greenberg, J., Harley, P., Grace, J., Malhi, Y., and Guenther, A.: Effect of drought on isoprene emission rates from 590 leaves of *Quercus virginiana* Mill. *Atmos. Environ.*, 38, 6149–6156, doi: 10.1016/j.atmosenv.2004.07.028, 2004b.

Peñuelas, J., and Staudt, M.: BVOCs and global change. *Trends Plant Sci.*, 15, 133–144, doi: 10.1016/j.tplants.2009.12.005, 2010.

R Core Team. R: A Language and Environment for Statistical Computing. R foundation for statistical Computing: Vienna, Austria, 2017.

Rennenberg, H., Loreto, F., Polle, A., Brilli, F., Fares, S., Beniwal, R. S., and Gessler, A.: Physiological responses of forest trees to heat and drought. *Plant Biol.*, 8, 556–571, doi: 10.1055/s-2006-924084, 2006.

595 Rombach, J.: Einfluss reduzierter Wasserverfügbarkeit auf die VOC-Emissionen bei Buchen, Albert-Ludwigs Universität, Freiburg, 13, 14, doi: 10.1186/s13007-017-0166-6, 2018.

Sander, R.: Compilation of Henry's law constants (version 4.0) for water as solvent. *Atmos. Chem. Phys.*, 15, 4399–4981, doi: 10.5194/acp-15-4399-20, 2015.

600 Saunier, A., Ormeño, E., Wortham, H., Temime-Roussel, B., Lecareux, C., Boissard, C., and Fernandez, C.: Chronic drought decreases anabolic and catabolic BVOC emissions of *Quercus pubescens* in a Mediterranean forest. *Front. Plant Sci.*, 8, 71, doi: 10.3389/fpls.2017.00071, 2017.

Scholander, P. F.: The role of solvent pressure in osmotic systems. *P. Natl. Acad. Sci.*, 55, 1407–1414, 1966.

Schönwiese, C.D.: Praktische Statistik für Meteorologen und Geowissenschaftler. 6. ed., Bornträger, Stuttgart, Germany, 302 p., ISBN-13: 978-3443010577, 2006.

605 Seinfeld, J. H., and Pandis, S. N.: Atmospheric Chemistry and physics: From air pollution to climate change. 3rd ed., Wiley Intersci., Hoboken, p.1152, ISBN: 978-1-118-94740-1, 2016.

Šimpraga, M., Verbeeck, H., Demarcke, M., Joó, É., Pokorska, O., Amelynck, C., Schoon, N., Dewulf, J., van Langenhove, H., Heinesch, B., Aubinet, M., Laffineur, Q., Müller, J.-F., and Steppe, K.: Clear link between drought stress, photosynthesis and biogenic volatile organic compounds in *Fagus sylvatica* L. *Atmos. Environ.*, 45, 5254–5259, doi: 10.1016/j.atmosenv.2011.06.075, 2011.

610 US EPA: Estimation Programs Interface Suite™ for Microsoft Windows, v. 4.11 or insert version used]. United States Environmental Protection Agency, Washington, DC, USA, 2018. (<https://www.epa.gov/tsca-screening-tools/download-epi-suitetm-estimation-program-interface-v411>), 2018.

van Genuchten, M. T.: A closed-form equation for predicting the hydraulic conductivity of unsaturated soils. *Soil Sci. Soc. Am. J.*, 44, 892–898, 1980.

615



Table 1. Overview of abbreviated terms and parameter names

Abbreviation	name	Abbreviation	name
a, b, c	fitting parameters, indices 'g' and 'h' reflect growth and hydraulic conductivity based fits	NO_x	nitrogen oxides (=NO+NO ₂)
β	temperature dependent increase of emission rates	PAR	photosynthetically active radiation
CCN	cloud condensation nuclei	PWP	permanent wilting point
E	emission rate of compound (class) [mg g(dw) ⁻¹ h ⁻¹]	ROS	reactive oxidation species
E_0	emission rate at standard cond.	RSE	residual standard error
$FASW\%$	fraction of available soil water [%]	SAR	structure activity relationships
FK	field capacity	SM	soil moisture
$\gamma_T, \gamma_L, \gamma_{CO_2}, \gamma_{SM}$	emission regulating factor for the impact of T, light, CO ₂ and soil moisture	SQT	sesquiterpenes (C ₁₅ H ₂₄)
$\gamma_{SM,g}, \gamma_{SM,h}$	γ_{SM} described by growth or hydraulic conductivity curve	$SWA\%, SWA_v$	soil water availability, percentile [%] and volumetric [v]
k_{OH}, k_{O3}	reaction rate constants with OH and ozone	SWC_v, SWC_m	Soil water content volumetric [vol %] and by mass [mass %]
MT	monoterpenes (C ₁₀ H ₁₆)	VPD	vapour pressure deficit
nFK	net field capacity	ψ, ψ_{pd}	matrix or water potential [MPa]



625

Table 2. Overview of studies, tree species and corresponding conditions as well as soil water parameters used for deriving the gswc parameterization for isoprene, MT and SQT emissions. References to the individual studies are listed in the final column. Soil water status parameters include the fraction of available soil water (FASW in %), leaf water content, available soil water (SWA% in %), soil water content by volume (SWC_v), by mass (SWC_m) and by the ratio water volume per soil mass (SWC_{vm}), stem diameter and water potential during daytime (ψ in MPa) and predawn (ψ_{PD} in MPa),

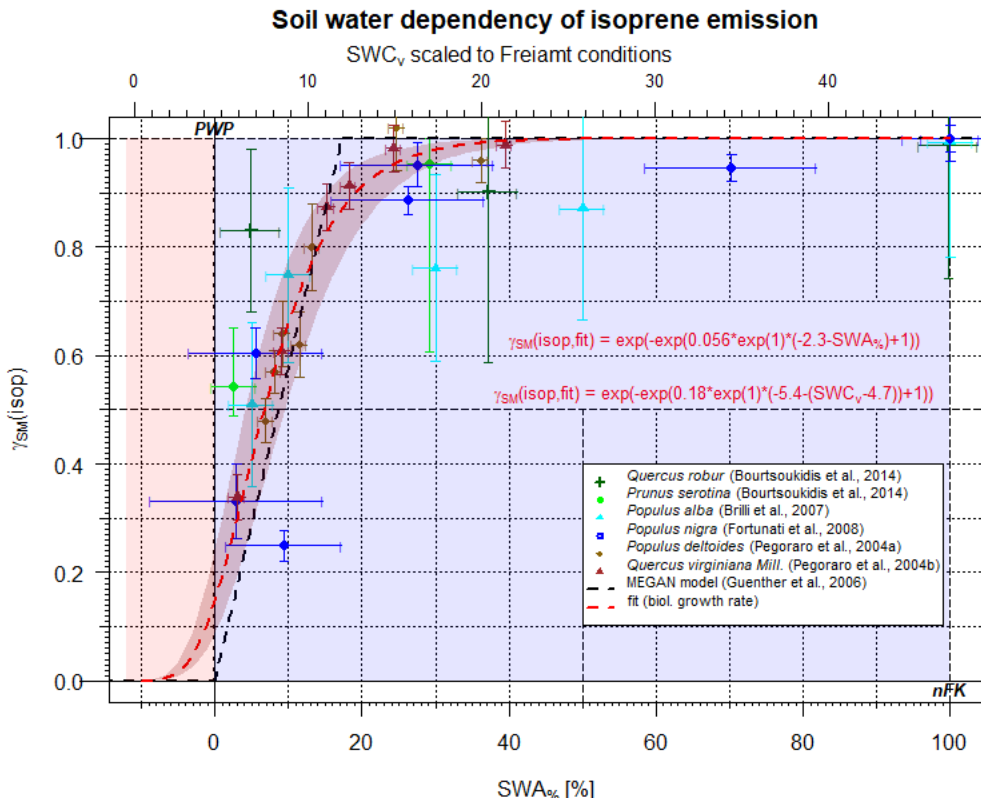
Tree species		Soil type	PWP ass. [m ³ m ⁻³]	VOC species classified	Parameter describing water status	Rewa- tering	environment	Reference
Lat. Name	engl. name							
<i>Castanea sativa</i>	sw. chestnut	70% sand, 30% humus?	2.8	different MTs	SWC _v	no	plant chamber	Lüpke et al., 2017a
<i>Cistus albidus</i>	rockrose	calcareous soil	6.7	MTs, SQTs	ψ , SWC _{vm}	no	pots, greenhouse?	Ormeno et al., 2007
<i>Cistus ladanifer</i>	common gum cistus	clay loam	10.2	Ox. MTs, MTs, SQTs, diterpenes	SWC _v , ψ	no	ambient	Haberstroh et al., 2018
<i>Cistus sinensis</i>	orange	clay loam	10.9	trans- β -ocimene (MT), β -carophyllene (SQTs)	SWC _v , ψ	yes	pot, greenhouse	Hansen and Seufert, 1999
<i>Fagus sylvatica</i>	European beech	CPS+fertilizer: 100% org?	6.0	total MTs	stem diameter	yes	growth room	Simpraga et al., 2011
<i>Fagus sylvatica</i>	European beech	Bedrock?	9.0±1.0	Isoprene, MTs, SQTs + 70 VOCs	Leaf water content, ψ_{PD} and ψ , SWC _v nearby	no	ambient	Rombach, 2018
<i>Pinus sylvestris</i>	pine	70% sand, 30% humus	2.8	1,8-cineole, different MTs	SWC _v	yes	plant chamber	Lüpke et al., 2017b
<i>Populus alba</i>	white poplar	CPS: 100% org	6.0	Isoprene	SWA%	yes	growth chamber	Brilli et al., 2007
<i>Populus deltoids</i>	cottonwo od	60% bare soil, 40% organic	7.4	Isoprene	SWC _v , ψ_{PD}	no	greenhouse	Pegoraro et al., 2004a
<i>Populus nigra</i>	black poplar	50% org., 50% sand	3.5	Isoprene	FASW%	yes	growth chamber	Fortunati et al., 2008
<i>Prunus serotina</i>	cherry	70%, 30%	4.7	MTs, SQTs, selected OVOCs	SWA%	no	greenhouse	Bourtsoukidis et al., 2014
<i>Rosmarinus off.</i>	rosemary	calcareous soil	6.7	MTs, SQTs	ψ , SWC%	no	pots, greenhouse?	Ormeno et al., 2007
<i>Quercus ilex</i>	oak	Silty clay loam	13.6	different MTs	ψ	yes	ambient	Lavoir et al., 2009
<i>Quercus robur</i>	oak	70%, 30%	4.7	MTs, SQTs, selected OVOCs	SWA%	no	greenhouse	Bourtsoukidis et al., 2014
<i>Quercus virginiana</i> Mill.	live oak	CPS: 100% org?	5.0	Isoprene	SWC _v , ψ_{PD}	no	phytotron	Pegoraro et al., 2004b

CPS: commercial potting soil (e.g. by Agrofino, Miracle Grow) including or plus fertilizer (Basacot)



Table 3. Change for individual mono- and sesquiterpene species emission fluxes of *Fagus sylvatica* for two SM conditions (Rombach, 2018). Because of not normal distributed data, values are stated as median and 25th (lower) and 75th (upper) percentiles.

Species	SWA% [%]		Total amount [$\mu\text{g g}(\text{dw}) \text{h}$]		Rel. amount [%]	
	A	B	A	B	A	B
monoterpenes	6₄⁸	3₁⁵	11.7_{2.9}^{35.7}	0.8_{0.4}^{2.4}	100	
Sabinene	6 ₄ ⁸	3 ₁ ⁵	11.2 _{2.6} ^{21.9}	0.2 _{0.1} ^{3.0}	91 ₇₉ ⁹⁵	37 ₂₃ ⁷⁵
Limonene	6 ₄ ⁸	3 ₁ ⁵	0.3 _{0.1} ^{1.3}	0.1 _{0.1} ^{0.3}	5 ₃ ⁹	12 ₈ ¹⁹
trans- β -ocimene	6 ₄ ⁸	3 ₁ ⁵	0.2 _{0.0} ^{1.2}	0.2 _{0.1} ^{0.9}	1 ₀ ¹⁰	39 ₁₀ ⁶⁴
sesquiterpenes	6₄⁸	3₁⁵	10.43_{2.88}^{17.23}	27.65_{12.12}^{42.27}	100	
isolongifolene	6 ₄ ⁸	3 ₁ ⁵	9.10 _{2.22} ^{15.57}	12.43 _{6.60} ^{30.17}	88 ₆₃ ⁹⁷	82 ₃₅ ⁹⁷
longifolene	6 ₄ ⁸	3 ₁ ⁵	0.39 _{0.15} ^{0.79}	0.30 _{0.20} ^{1.56}	4 ₂ ¹²	1 ₁ ⁶
α -farnesene	6 ₄ ⁸	3 ₁ ⁵	0.34 _{0.05} ^{0.57}	2.64 _{0.21} ^{6.56}	3 ₁ ⁷	9 ₁ ⁴⁹
Junipene	6 ₄ ⁸	3 ₁ ⁵	0.12 _{0.04} ^{0.15}	0.06 _{0.04} ^{0.50}	1 ₁ ²	1 ₀ ⁶
α -bergamotene	6 ₄ ⁸	3 ₁ ⁵	0.05 _{0.02} ^{0.07}	0.29 _{0.05} ^{0.77}	0 ₀ ¹	1 ₀ ⁶

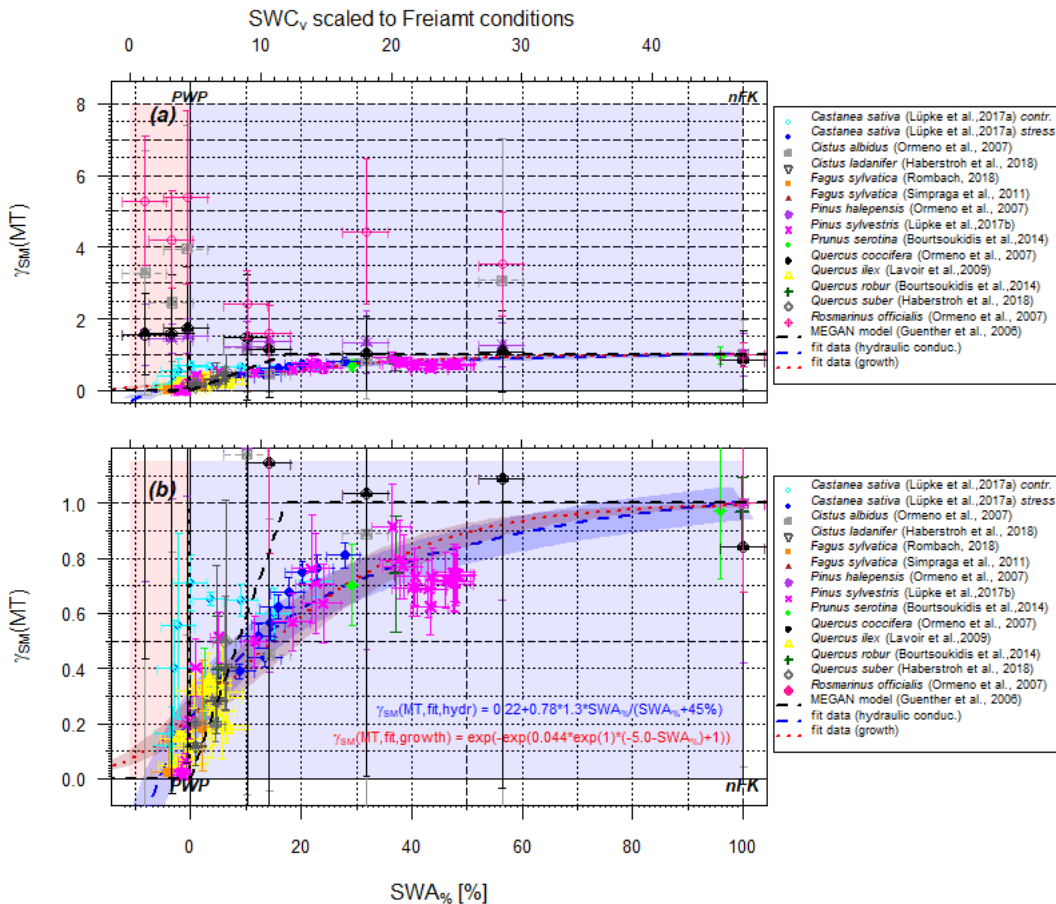


630

Figure 1: Scaling parameter $\gamma_{SM}(\text{isop})$ for the effect of soil moisture on isoprene emissions as a function of SWA% (lower x-axis) and for comparison the SWC_v for a selected condition (upper horizontal axis). Data points represent observations, and different colours refer to different studies. The black dashed line displays the approach by Guenther et al. (2006; 2012), the red one the present form.



Soil water dependency of total monoterpene emission



635

Figure 2: Scaling parameter $\gamma_{SM}(MT)$ for the effect of soil moisture on total MT emissions as a function of SWA% (lower x-axis) and for comparison the SWC_v for a selected condition (upper horizontal axis). The upper plot (a) displays the full data range, while the lower plot (b) zooms vertical area between 0 and 1.2. Data points represent observations, and different colours refer to different studies. The black dashed line displays the approach by Guenther et al. (2006; 2012), the red one the present form using hydraulic conductivity as driving force and the darkred one the biological growth stress as driving force.

640

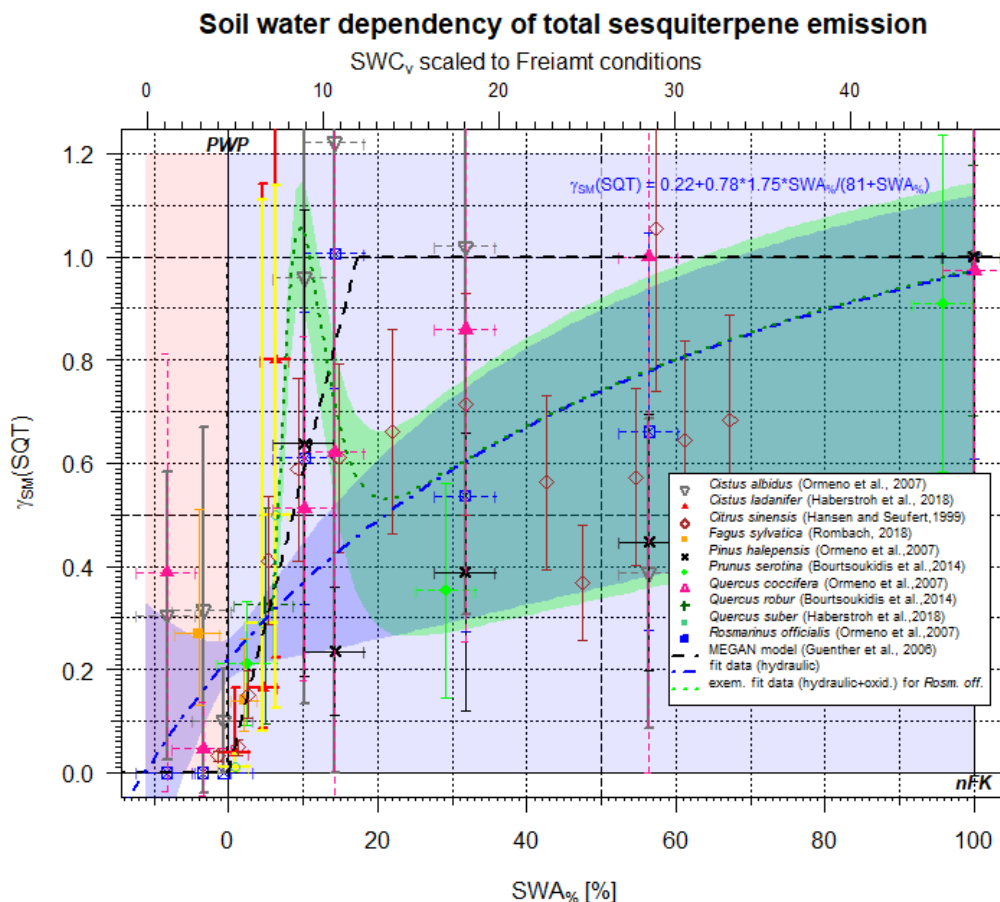
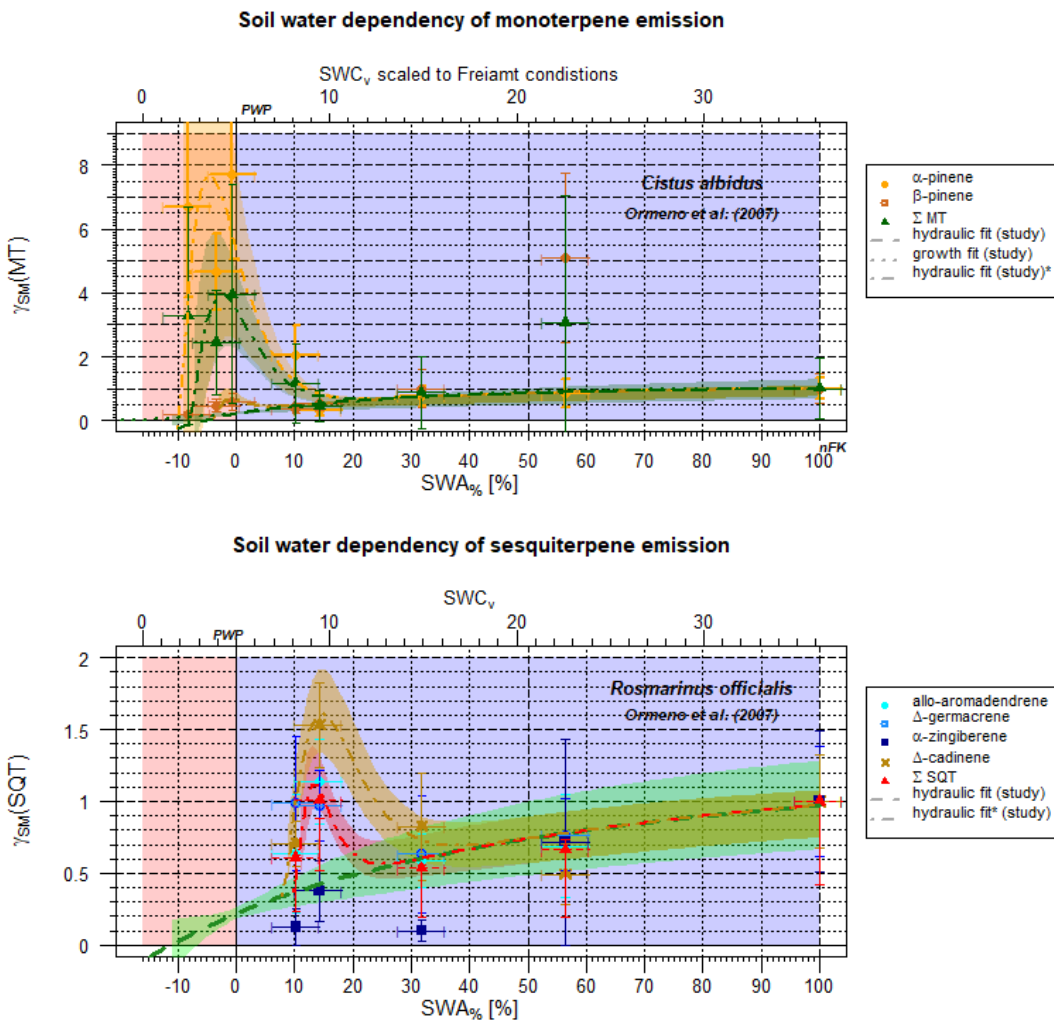


Figure 3: Scaling parameter $\gamma_{SM}(SQT)$ for the effect of soil moisture on SQT emissions as a function of SWA% (lower x-axis) and for comparison the SWC_v for a selected condition (upper horizontal axis). Data points represent observations, different colours refer to different studies. The black dashed line displays the approach by Guenther et al. (2006; 2012), the blue one the present form. The green pointed line represents an exemplary fit to $\gamma_{SM}(SQT)$ based on *Cistus* and *Rosmarinus officinalis* data.



650

Figure 4: Exemplary scaling parameter γ_{SM} for the effect of soil moisture with a maximum at PWP on individual and total terpene emissions as a function of SWA % (lower x-axis), and for comparing the SWC_v at Freiamt soil conditions (upper horizontal axis) (*Cistus albidus*) (Ormeno et al., 2007). Top plot: SM effect on monoterpene emission fluxes of individual structured monoterpenes, as well as of the total sum of monoterpenes; lower plot: the same for individual structures and total sum of sesquiterpene emissions (*Rosmarinus officinalis*) (Ormeno et al., 2007).

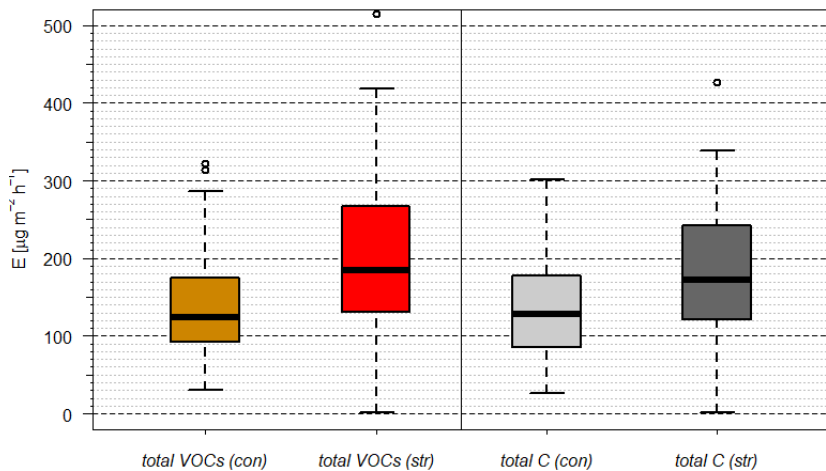
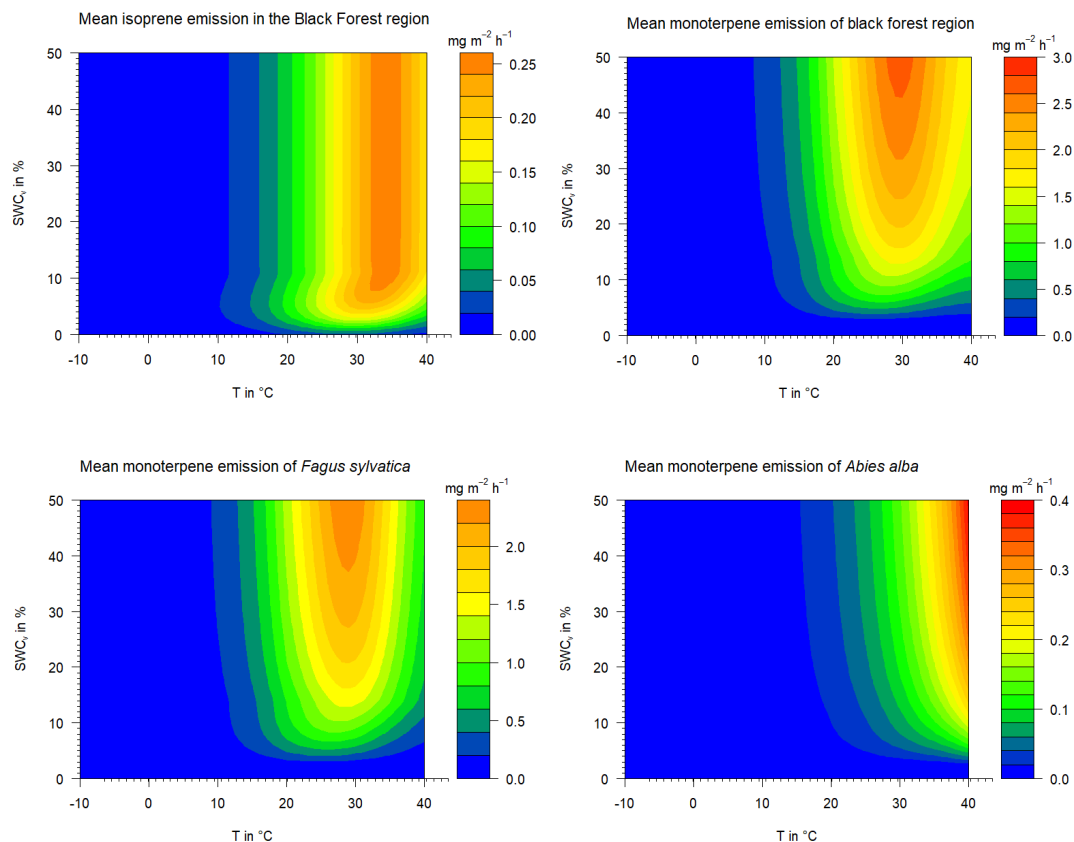


Figure 5: Change for individual mono- and sesquiterpene species emission fluxes of *Fagus sylvatica* for two SM conditions
655 (Rombach, 2018). Because of not normal distributed data, values are stated as median and 25th (lower) and 75th (upper) percentiles.



660 **Figure 6: Mean isoprene and monoterpene emissions under different temperature and drought stress conditions. “Black Forest region” represents the forest inventory mean tree species mixture of the Black Forest area. Upper left: total Isoprene emission, upper right: total monoterpene emission, baseline: *Fagus sylvatica* and *Abies alba* based MT emission rates (lower left and right).**

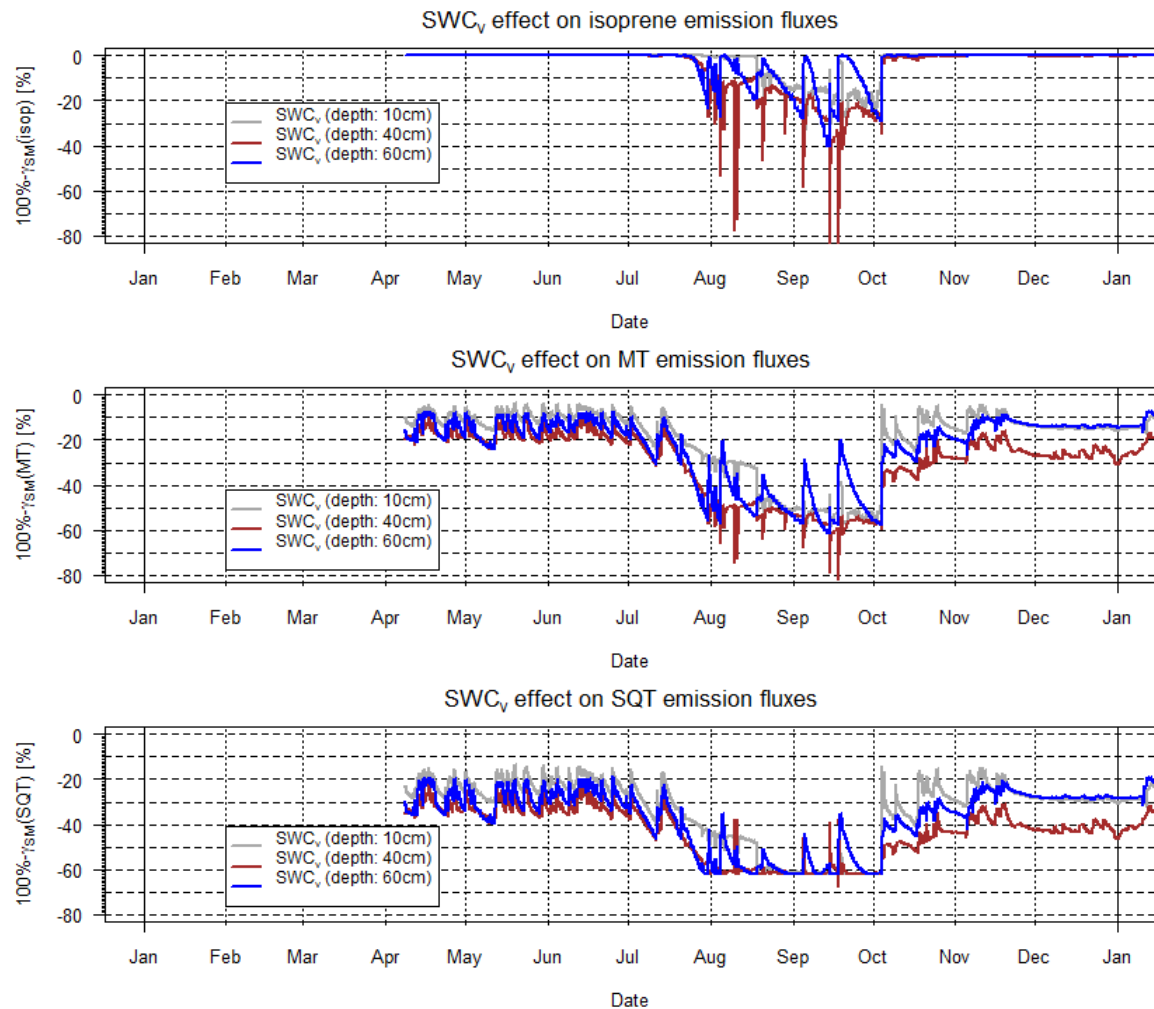


Figure 7: Calculated γ_{SM} effects during 2016 at Freiamt on isoprene, total MT and SQT emission rates. Note, two induced drought periods during summer and quite saturated conditions else when.
 665